Bull. Mater. Sci., Vol. 30, No. 6, December 2007, pp. 595–600. © Indian Academy of Sciences.

Role of Ti_3Al/silicides on tensile properties of Timetal 834 at various temperatures

K V SAI SRINADH[†], NIDHI SINGH[††] and V SINGH*

Department of Metallurgical Engineering, Institute of Technology, Banaras Hindu University, Varanasi 221 005, India
[†]Department of Mechanical Engineering, National Institute of Technology, Warangal 506 004, India
[††]National Metallurgical Laboratories Madras Centre, CSIR Madras Complex, Chennai 600 013, India

MS received 22 February 2007; revised 15 October 2007

Abstract. **Extremely fine coherent precipitates of ordered Ti_3Al and relatively coarse incoherent precipitates of S_2 silicide exist together in the near α-titanium alloy, Timetal 834, in the dual phase matrix of primary α and transformed β. In order to assess the role of these precipitates, three heat treatments viz. WQ, WQ–A and WQ–OA, were given to have no precipitates, Ti_3Al and silicide and only silicide precipitates in the respective conditions. Tensile properties in the above three heat treated conditions were determined at room temperature, 673 K and 873 K. It was observed that largely Ti_3Al precipitates were responsible for increase in the yield strength and decrease in ductility in this alloy.**

Keywords. **Near α-titanium alloy; Timetal 834; Ti_3Al/silicide precipitates; tensile properties.**

1. Introduction

Near α-titanium alloys have been designed for high temperature application as compressor discs of advanced gas turbines in jet engines. It has been established in the near α-titanium alloy, Timetal 834, that precipitation of the ordered Ti_3Al (α_2) phase and silicides occurs on slow cooling in air/furnace but not during quenching in water/oil, following solution treatment in the $\alpha + \beta$ phase field (Singh 2000). However, precipitation of these phases occurs even in the rapidly quenched samples from the stabilization treatment at 973 K for 2 h, followed by cooling in air (Singh 2000). On the other hand, coarsening of the Ti_3Al and silicide precipitates, preexisting in the slow cooled specimens, occurs during stabilization treatment of the slow cooled specimens. Thus, there is a combined effect of Ti_3Al and silicide precipitates on the observed mechanical properties of the alloy, Timetal 834, in the stabilized condition. Recently, Kumar *et al* (2003) studied LCF behaviour of this alloy in water quenched as well as in water quenched and stabilized condition, at room temperature and observed lower fatigue resistance in the stabilized condition where there were precipitates of Ti_3Al and silicides. The lower fatigue resistance in the stabilized condition, with Ti_3Al/silicide precipitates, has been attributed to detrimental role of the coherent precipitates of Ti_3Al, in promoting localization of plastic strain by planar slip due to their shearing and consequent enhancement in the process of fatigue crack initiation.

Madsen and Ghonem (1995) identified separate effects of the Ti_3Al and silicide precipitates, on tensile properties and fatigue crack growth behaviour of the near α-Ti 1100 alloy at room temperature and 866 K. They found that Ti_3Al precipitates were largely responsible for increase in the yield strength and decrease in ductility both at room temperature as well as at 866 K. On the other hand, increase in the rate of fatigue crack growth at room temperature was associated essentially with silicide precipitates and there was only minor role of Ti_3Al precipitates. However, at 866 K, there was slight improvement in the resistance against fatigue crack propagation and this too was attributed to silicide precipitates. They also observed that decrease in ductility was more pronounced at room temperature than at 866 K and the appearance of serrations, associated with dynamic strain aging, was suppressed in the aged specimens, likely due to depletion of silicon from the solid solution, due to precipitation of silicides (Madsen and Ghonem 1994). Woodfield *et al* (1988), on the other hand, had shown that reduction in ductility of the alloy, Ti-5331S (also known as IMI829) at room temperature was essentially due to silicides. The loss in ductility resulting from silicides was found to be associated with fracture of silicide particles and consequent formation of intense slip bands. Presence of ordered Ti_3Al and S_2 silicide $[(TiZr)_6Si_3]$ has been reported in the alloy, Timetal 834, following solution treatment in the $\alpha + \beta$ phase, water/oil quenching and aging at 973 K for 4 h (Cope and Hill 1988) and 24 h (Ramachandra *et al* 1993).

The present investigation deals with the role of Ti_3Al and silicide precipitates on tensile properties of the alloy,

*Author for correspondence (vakil@bhu.ac.in)

Table 1. Details of the heat treatment given to alloy, Timetal 834, following solution treatment in the ($\alpha + \beta$) phase field at 1283 K and quenching in water.

Designation	Aging treatment	Precipitates
WQ (Water quenched)	Nil	Nil
WQ–A (Water quenched and aged)	Aged at 973 K for 2 h and cooled in air (Commercial stabilization treatment)	Ti_3Al + silicides
WQ–OA (Water quenched and over aged)	Aged at 1098 K for 2 h and quenched in water	Only silicides

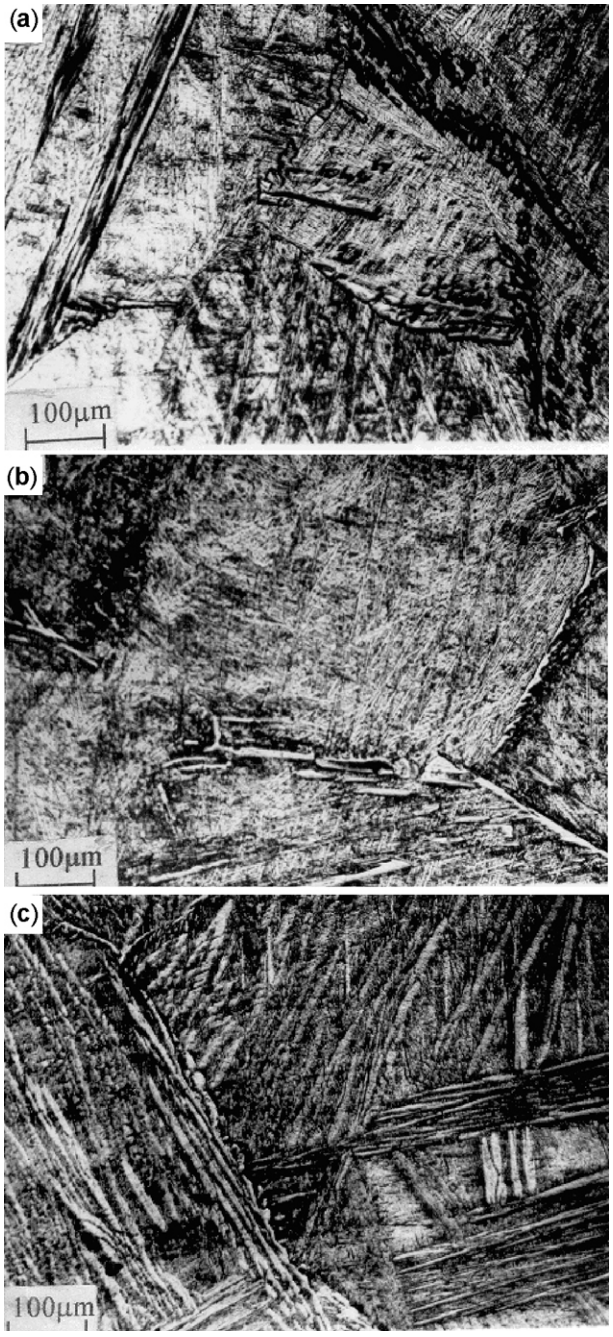

Figure 1. Optical micrographs showing microstructure of the alloy, 834, in different heat treated conditions (**a**) WQ, (**b**) WQ–A and (**c**) WQ–OA conditions.

Timetal 834, at room temperature, 673 K and 873 K by designing suitable heat treatments. It is observed that Ti_3Al precipitates play a dominant role both on strength and ductility of this alloy.

2. Experimental

Alloy, Timetal 834, was supplied by the Aeronautical Materials Testing Laboratory (AMTL), Hyderabad, in the form of rods of 18 mm diameter in the ($\alpha + \beta$) solution treated, air cooled and stabilized condition. It was imported from M/s Timetal Industry, UK. It contained 5·07 Al, 3·08 Sn, 3·45 Zr, 0·66 Nb, 0·31 Mo, 0·2 Si, 0·04 C, 0·105 O, 0·0025 N, 0·004 H and balance Ti (wt%). Blanks of 100 mm length and 18 mm diameter were longitudinally sectioned into four quadrants of nearly equal cross sections. Subsequently these were machined into a cylindrical cross-section of 7 mm diameter. The cylindrical blanks of 7 mm diameter were vacuum ($\approx 10^{-3}$ torr) sealed in silica tube with titanium getter, solution treated in the β phase field at 1353 K for 30 min, and cooled to 1283 K in the $\alpha + \beta$ phase field. These blanks were kept at this temperature for 1 h and subsequently quenched in water. Solution treatment in the β phase field was given to dissolve silicide precipitates, if any. Some of the water quenched blanks were again vacuum sealed in silica tube and subjected to two different aging treatments, separately (table 1).

Specimens for optical metallography were mechanically polished on emery papers of 1/0 to 4/0 grades. Final polishing was carried out on sylvet cloth, mounted on a smooth rotating polishing wheel, using water suspensions of alumina powder of different grades. Polished samples were etched with a solution of 10 HF + 5HNO_3 + 85H_2O (volume percent) at room temperature and the microstructures were examined using Metalux-3 optical microscope. The internal microstructural details were examined by JEOL 200 CX transmission electron microscope. TEM foils were prepared by electrolytic polishing of thin discs of 3 mm diameter, punched from thin sections of ~50 μm thickness. Electropolishing was carried out in an electrolyte containing 59% methanol, 35% *n*-butanol and 6% perchloric acid (by volume), at 15 V, using a twin jet polisher. The temperature of the electrolyte was maintained at or

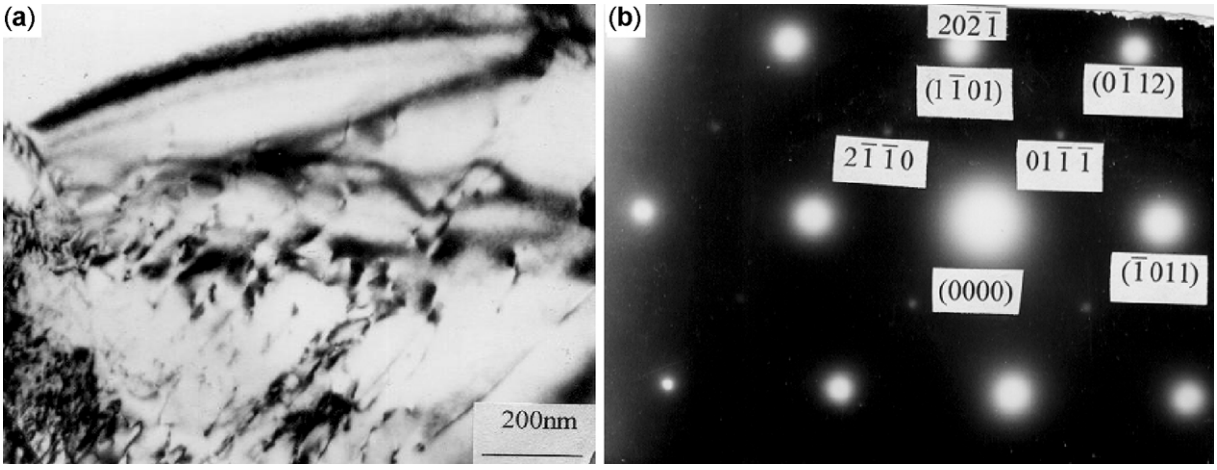

Figure 2. (**a**) Bright field transmission electron micrograph of the alloy, Timetal 834, in WQ–A condition and (**b**) selected area diffraction pattern $[01\bar{1}1]$ α_p//$[01\bar{1}2]$ $\alpha 2$.

Table 2. Tensile properties of the alloy, Timetal 834, in WQ, WQ–A and WQ–OA conditions at RT, 673 K and 873 K.

Designation	Temp. (K)	YS (MPa)	UTS (MPa)	UE (%)	TE (%)	RA (%)	σ_{UTS}/σ_{YS}	n	K (MPa)	VHN
WQ	RT	987	1128	6·03	7·5	7·5	1·14	0·05	1395	376
	673	660	837	9·09	12·5	15	1·26	0·06	1029	
	873	560	695	8·40	18·0	30	1·24	0·08	955	
WQ–A	RT	1028	1134	5·2	6·5	8	1·10	0·05	1410	402
	673	677	862	9·8	16·0	20	1·27	0·06	1052	
	873	567	702	15·0	21·0	35	1·23	0·08	978	
WQ–OA	RT	980	1098	6·9	7·5	7·5	1·12	0·05	1275	370
	673	624	767	6·4	12·5	15·0	1·22	0·08	998	
	873	538	666	5·1	12·0	15·0	1·23	0·06	860	

little below 233 K, using liquid nitrogen, throughout the process of electrothinning.

Cylindrical tensile specimens of gauge length, 15·4 mm and gauge diameter, 4·5 mm, were machined from the above heat-treated blanks and tested in tension using Instron of 50 KN capacity at a nominal strain rate of $5{\cdot}6 \times 10^{-4}$ s^{-1}. Tests at high temperature were performed using a split type electric resistance-heating furnace. Fracture behaviour of the specimens was examined under JEOL scanning electron microscope (840A).

3. Results

3.1 *Microstructure*

Optical microstructure of the alloy, Timetal 834, in the unaged, peak aged and over aged conditions are shown in figures 1a, b and c, respectively. It may be seen that, in general, the microstructures are alike and show large β grains transformed into α platelets, though there is variation in size of the α platelets. Such variation in the size of α platelets occurs from one to other region. The microstructure of the alloy, 834, in the WQ–A condition is shown by the transmission electron micrograph in figure 2. The size of the Ti_3Al precipitates is very small and hence they are not seen clearly in the bright field micrograph (figure 2a), however, the diffraction spots corresponding to the ordered Ti_3Al precipitates are clearly seen in the diffraction patterns (figure 2b).

3.2 *Tensile properties*

Tensile properties of the alloy, Timetal 834, in the three heat-treated conditions are summarized in table 2. It may be seen that there is appreciable difference in tensile properties of the material in different heat-treated conditions. Both strength as well as ductility parameters are affected by heat treatment and test temperature. The tensile stress–strain curves in the different heat-treated conditions, tested at room temperature, 673 K and 873 K, are shown in figure 3. It is obvious that there is difference in the levels of the stress–strain curves in the three heat treated conditions, at all the three test temperatures. The level of the stress–strain curve of the peak aged (WQ–A) material is highest whereas that of the over aged (WQ–OA) one is lowest and the level of the unaged (WQ) ma-

terial lies between these two, at all the three test temperatures. Further, it may be seen that ductility of the alloy, in all the three heat-treated conditions, increases with increase in temperature from room temperature to 873 K. The values of the yield strength, tensile strength, uniform elongation (UE), total elongation (TE), work hardening parameters (n and K) and the hardness, for the three heat treated conditions, at room temperature, 673 K and 873 K are presented in table 2. The degree of work hardening (σ_{UTS}/σ_{YS}) increases with test temperature for all the three conditions. In general, while the work hardening exponent (n) increases with increase in temperature, there is opposite trend in variation of the strength factor (K).

Fracture behaviour of the unaged (WQ) and peak-aged (WQ–A) specimens tested at room temperature and 873 K was examined by SEM. The fracture characteristics are displayed in figure 4. It is obvious from the fractographs that, in general, the fracture is transgranular and ductile in nature. While the dimples on fracture surface of the WQ material, tested at room temperature, are fine and shallow (figure 4a), those of the WQ specimen, tested at 873 K (figure 4b), are larger in size and depth. The morphology of the dimples on fracture surface of the WQ–A specimen, tested at room temperature, is quite different and the dimples are elongated (figure 4c). However, the dimples on fracture surface of the WQ–A specimen tested at 873 K, are relatively less elongated and may be seen to be equiaxed in some regions (figure 4d).

4. Discussion

The fine microstructural features of the WQ–A material is shown by the bright field transmission electron micrograph in figure 2(a). Nearly parallel α platelets, resulting from transformation of the metastable β, may be seen in the lower region. The diffraction spots corresponding to Ti_3Al precipitates are indexed and displayed in figure 2(b). The occurrence of Ti_3Al and S_2 [$(TiZr)_6Si_3$] silicide precipitates in the peak aged condition, ($\alpha + \beta$) ST–WQ–A, has been established earlier (Singh 2000). Presence of Ti_3Al and S_2 silicide has also been established in the ($\alpha + \beta$) solution treated and water quenched material following aging in the temperature range 873 to 973 K for 24 h (Ramachandra *et al* 1993). The role of Ti_3Al precipitates in enhancing planarity of slip, during low cycle fatigue (LCF) of the alloy, Timetal 834, at room temperature as well as 873 K has been established earlier (Singh *et al* 2002, 2007).

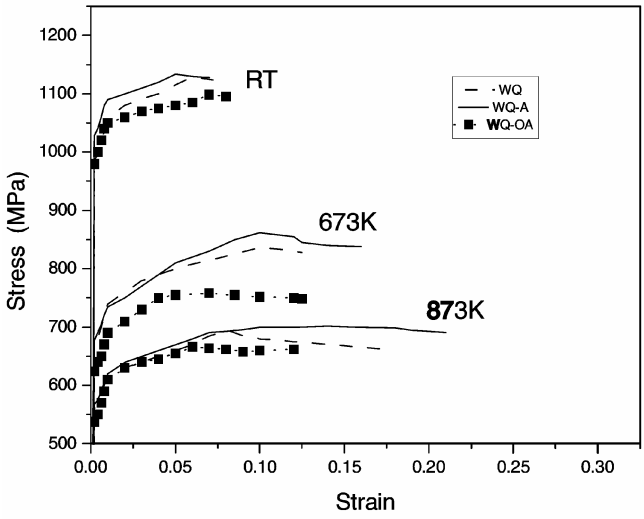

Figure 3. Tensile stress–strain curves of the alloy, Timetal 834, in WQ–A and WQ–OA conditions, at RT, 673 K and 873 K.

The highest strength of the alloy, 834, in the peak-aged condition (WQ–A) is naturally due to presence of the coherent ordered precipitates of Ti_3Al, in agreement with the earlier investigations (Madsen and Ghonem 1994, 1995). The primary α as well as the α lamellae of transformed β are hardened by precipitation of extremely fine Ti_3Al precipitates (~5 nm) resulting from ageing at 973 K for 2 h (Andres *et al* 1997). The degree of hardening caused by Ti_3Al precipitates is higher in the primary α than that in the α lamella due to partitioning effect of the alloying elements, during the recrystallization treatment in the ($\alpha + \beta$) phase field (Neal 1995; Andres *et al* 1997). Ti_3Al precipitates are known to grow slowly and remain coherent even up to the size of 120 nm. The role of the fine incoherent precipitates of S_2 silicides on strength of the alloy, 834, in this heat-treated condition would only be minor, if any. It may be observed that both yield strength and tensile strength are lower in the over aged condition of the alloy, 834, in the present investigation, where there are only S_2 silicide precipitates.

The yield and tensile strengths of the material in the over aged condition are lower than those of the unaged one, at room temperature. This may be understood in terms of ineffective role of the coarse incoherent silicide precipitates on strengthening coined with decrease in solid solution strengthening due to depletion of silicon as well as Zr, the potential solid solution strengtheners, from the matrix. It may be seen from table 2 and figure 3 that nearly similar trend is followed in relative yield strengths and tensile strengths of the unaged, peak aged and overaged materials also at the higher test temperatures of 673 K and 873 K.

The ductility of the peak-aged material, with coherent Ti_3Al precipitates and incoherent S_2 silicide precipitates, is lower than that of the over aged one, containing exclusively incoherent S_2 silicide precipitates, at room temperature (table 2). Thus, it is obvious that this is due to detrimental role of the coherent precipitates of Ti_3Al. This effect of coherent Ti_3Al precipitates on ductility of the peak aged material, may be attributed to enhanced planarity of slip resulting from shearing of the fine coherent

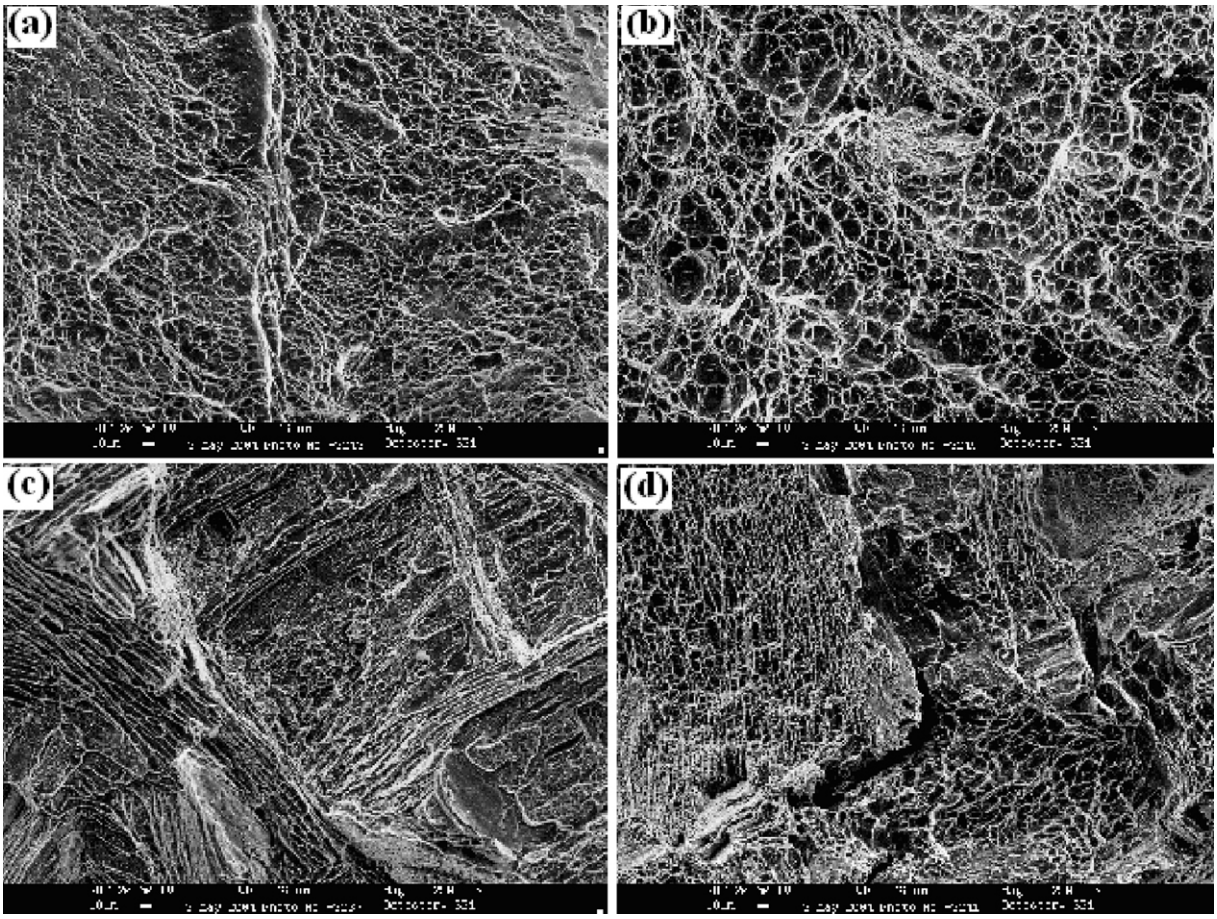

Figure 4. SEM fractographs showing fracture behaviour of the alloy, Timetal 834, tested in tension (**a**) WQ, RT, (**b**) WQ, 873 K, (**c**) WQ–A, RT and (**d**) WQ–A, 873 K.

Ti_3Al precipitates. The loss in ductility of the alloy, 834, due to Ti_3Al precipitates in the present investigation, is in line with the earlier observation made in the near α-Ti alloy, Ti-1100 (Madsen and Ghonem 1994, 1995).

It is interesting to observe that ductility of the peak aged material increases with temperature and also is more than those of the unaged and over aged ones at both 673 K and 873 K. It may be understood in terms of increased stability of the Ti_3Al precipitates due to rapid reordering of the sheared Ti_3Al precipitates (Gysler and Weissmann 1977). Thus, the deformation by slip becomes more homogeneous with increase in temperature. It may be seen that at 873 K, ductility of the peak-aged material is highest, whereas that of the over aged material is lowest among the three conditions. It may be attributed to activation of additional slip systems in the Ti_3Al phase, than that at the test temperature of 673 K. Thus, the tendency of enhanced planarity of slip, observed at room temperature in the peak aged condition, is reduced at elevated temperature and the fracture surface shows less faceting and more well defined equiaxed dimples (figure 4d). The role of coarse silicide precipitates, in the overaged condition, may be seen to be detrimental on ductility at 873 K, in agreement with the earlier observation made in the alloy, 829 (Neal and Blenkinsop 1980), which is very close to 834. The coarse silicide particles are relatively brittle compared with the matrix and promote void initiation in tensile testing when planar arrays of dislocation meet the silicide particles. This is known to affect 'reduction in area' more than 'elongation' (Neal and Blenkinsop 1980).

5. Conclusions

(I) Alloy, Timetal 834, exhibits highest strength in the WQ–A condition, containing coherent ordered precipitates of Ti_3Al and fine incoherent particles of silicide at room temperature, 673 K and 873 K.

(II) Ordered Ti_3Al precipitates in the alloy, 834, exert detrimental effect on ductility of the alloy at room temperature due to enhanced planarity of slip. However, the detrimental effect of Ti_3Al on ductility disappears at elevated temperatures.

(III) Coarse silicide precipitates in the over aged condition cause reduction in ductility at 873 K.

References

Andres C, Gysler A and Lutjering G 1997 *Z. Metallkd* **88** 197

Cope M T and Hill M J 1988 *6th World conference on titanium, Conf. proc.* (eds) P La Combe *et al* (Cedex, France: Les Editions de physique, Les ulis) **1** p. 153

Gysler A and Weissmann S 1977 *Mater. Sci. Eng.* **27** 181

Kumar Amit, Singh Nidhi and Singh Vakil 2003 *Mater. Charact.* **51** 225

Madsen A and Ghonem H 1994 *Mater. Sci. & Eng.* **A177** 63

Madsen A and Ghonem H 1995 *J. Mater. Eng. & Perf.* **4** 301

Neal D F and Blenkinsop P A 1980 *Titanium Sci. & Technol.* **2** 1287

Ramachandra C, Singh A K and Sarma G M K 1993 *Metall. & Mater. Trans.* **A24** 1273

Singh Nidhi 2000 *Microstructure, tensile properties and LCF behaviour of titanium alloy, IMI 834*, Ph.D. Thesis, Banaras Hindu University, Varanasi

Singh Nidhi, Gouthama and Singh Vakil 2002 *Mater. Sci. & Eng.* **A325** 324

Singh Nidhi, Gouthama and Singh Vakil 2007 *Int. J. Fatigue* **29** 843

Woodfield A P, Postans P J, Loretto M H and Smallman R E 1988 *Acta Metall.* **36** 507